ISSN: 0067-2904

Numerical Simulation of Solar Granulation Dynamics Using Optical Correction Techniques

Huda Shaker Ali
Department of Astronomy and Space, College of Science, University of Baghdad, Baghdad, Iraq

Received: 22 /1 /2024 Accepted: 18 /5 /2024 Published: 30/4/2025

Abstract

High-resolution imaging of celestial bodies, especially the sun, is essential for understanding dynamic phenomena and surface details. However, the Earth's atmospheric turbulence distorts the incoming light wavefront, which poses a challenge for accurate solar imaging. Solar granulation, the formation of granules and intergranular lanes on the sun's surface, is important for studying solar activity. This paper investigates the impact of atmospheric turbulence-induced wavefront distortions on solar granule imaging and evaluates, both visually and statistically, the effectiveness of Zonal Adaptive Optics (AO) systems in correcting these distortions. Utilizing cellular automata for granulation modelling and Zonal AO correction methods, the study aims to understand system behavior under varying atmospheric turbulence conditions and provide recommendations for Zonal AO system enhancement for solar observations. Performance metrics, including Strehl Ratio, Correction Stability, Root Mean Squared Error (RMSE), and Correction Rate, were used to assess system performance under varying turbulence levels. However, challenges arise with increasing turbulence strength, impacting correction precision, stability, and speed. The results showed the weakness of the Zonal AO in treating high distortions in wavefront, as is evident by the decreases in Strehl Ratio values from 0.98 to 0.085 for disturbance strength values from 0.2 to 1, respectively.

Keywords: Zonal Adaptive Optics, Cellular Automata, Strehl Ratio, Kolmogorov Turbulence, PSF.

المحاكاة العددية لديناميكيات التحبيب الشمسي باستخدام تقنيات التصحيح البصري

هدى شاكر علي
قسم الفلك و الفضاء, كلية العلوم, جامعة بغداد, بغداد, العراق

الخلاصة

يعد التصوير عالي الدقة للأجرام السماوية وخاصة الشمس ضروريًا لفهم الظواهر الديناميكية وتفاصيل السطح . ومع ذلك فإن الاضطرابات الجوية للأرض تشوه جبهة موجة الضوء القادم . مما يشكل تحدي أمام التصوير الشمسي الدقيق . التحبيب الشمسي و تكوين الحبيبات والممرات الحبيبية على سطح الشمس مهم لدراسة النشاط الشمسي. يبحث هذا البحث في تأثير تشوهات جبهة الموجة الناجمة عن الاضطرابات الجوية

Email: hudashaker2000@gmail.com

على تصوير الحبيبات الشمسية وتقيم، بصريًا وإحصائيًا، فعالية أنظمة البصريات التكيفية المنطقية (AO) في تصحيح هذه التشوهات . تهدف هذه الدراسة باستخدام الأتمتة الخلوية لنمذجة التحبيب وطرق تصحيح Zonal AOإلى فهم سلوك النظام في ظل ظروف الاضطرابات الجوية المختلفة وتقديم توصيات لتحسين نظام Zonal AO لعمليات الرصد الشمسي . تم استخدام مقاييس الأداء بما في ذلك نسبة Strehl واستقرار التصحيح ومتوسط الجذر التربيعي للخطأ (RMSE) ومعدل التصحيح لتقييم أداء النظام في ظل مستويات اضطراب مختلفة . مع ذلك تنشأ تحديات مع زيادة قوة الاضطراب مما يؤثر على دقة التصحيح والاستقرار والسرعة . حيث أظهرت النتائج ضعف Zonal AO في معالجة التشوهات العالية في جبهة الموجة ويتضح ذلك من انخفاض قيم Strehl Ratio من 0.98 إلى 0.085 لقيم قوة الاضطراب من 0.2 إلى 1 على التوالي.

الكلمة المفتاحية: البصريات التكيفية النطاقية، الأتمتة الخلوية، نسبة Strehl، اضطراب Kolmogorov، PSF.

1-Introduction

Studying celestial bodies, especially the sun, requires high-resolution imaging for the purpose of comprehending the dynamic phenomena as well as the intricate surface details. Nonetheless, due to the fact that the Earth's turbulent atmosphere distorts the incoming light, there is a difficulty to the accurate detection of the solar characteristics from the sun's images. The production of granules and inter-granular lanes on the sun’s surface is referred to as solar granulation, and it is one of the significant fields of study in solar physics [1, 2]. Understanding those dynamic phenomena can result in a highly decreasing solar activity complexity. In the case of observing granulation patterns, atmospheric turbulence often leads to distortions that limit the solar imaging systems’ accuracy. AO systems seem as a potential solution for such issues and an improvement over the solar observations [3, 4].

AO systems’ performance that is intended for solar observations has been examined in that context, with an emphasis on how well those systems could reduce the wavefront distortions that are brought on by the atmospheric turbulence [5, 6]. In the present study, the solar granules’ dynamic behaviour is modelled by utilizing simulations of cellular automata, and wavefront distortion corrections, which are performed subsequently with the use of advanced AO approaches. Understanding and refining AO methods for solar imaging represents the main goal, along with testing their effectiveness under a variety of conditions of atmospheric turbulence [7, 8]. Such modification types are important for the purpose of enhancing image quality and offering a more detailed understanding of solar activity and structure, which include granules, sunspots, and magnetic phenomena [9, 10]. This study provides a comprehensive examination of the Zonal AO correction approaches and it evaluates their effectiveness in reducing wavefront distortions that happen as a result of air turbulence. Metrics of evaluation, like correction Stability, RMSE, Correction Rate and Strehl Ratio, are estimated as well as part of the study so as to show system adaptability to various atmospheric turbulence levels. This research has the objective of assessing the system's performance in various turbulence conditions and providing insightful recommendations for Zonal AO system enhancement for the solar observations.

1-The Cellular Automata Method

Cellular Automata (CA) is considered as one of the most basic modelling methods that are developed for systems with spatial and temporal dependencies. This approach, which has its roots in the field of computer science, has first been conceptualized as a "calculating machine". Four fundamental components characterize CA [11, 12]:

1. **Domain:** This comprises discrete elements, known as cells, within the informatics context. Cells can possess arbitrary spatial dimensions and shapes relative to each other. While predominantly explored in two-dimensional systems with square, triangular, or hexagonal cell shapes, the literature also encompasses one-dimensional and three-dimensional variations.
2. **Inner Variables:** Every cell should have a uniform and discrete set of potential inner variables. All of the inner variables combined together in every cell make up the "configuration."
3. **Neighborhood Convention:** The neighborhood convention defines which cell directly interacts and usually corresponds to a local configuration within a given radius. It is noteworthy, nevertheless, that cells that are not locally adjacent might be regarded as neighbors. It is imperative that neighborhood specifications remain consistent throughout all cells.
4. **Update Rule:** This embodies the essential dynamics of the structure. A cell's inner variable could just be modified in an update step depending on its own state and the states of its neighboring cells. Depending on the model, the research landscape supports both sequential (one cell updated at a time per step) and parallel (a simultaneous update of all cells) implementations. One update step corresponds to a discrete time interval in the majority of applications.

Together, such components establish the operational dynamics and framework of CA, offering a flexible modelling approach that may be used in a wide range of fields and problem domains.

1-Wavefront Representations

Reducing phase aberrations is the main objective of the AO system, which aims to improve astronomical image quality considerably. This corrective procedure uses two different sensing approaches. The first method for reducing phase aberrations in an Adaptive Optics (AO) system involves a modal representation of the wavefront error. In the second method, the wavefront error is described at every point or zone across the aperture using a Zonal representation [13, 14]. This work uses the Zonal method to illustrate the phase aberration profile. This approach uses regular grid surfaces with randomly generated values that follow the Kolmogorov model of turbulence.

1-Kolmogorov Power Spectral Models

A valuable framework for comprehending energy transmission in this complex system is provided by the Kolmogorov turbulence model. According to this theory, energy gradually dissipates as it approaches smaller scales, starting at bigger scales where the majority of energy is contained. As the turbulent fluid separates into ever finer scales, kinetic energy is conserved through the cascade pattern of the energy transfer from larger to smaller scales. A well-known concept is the Kolmogorov spectrum, which provides a basic power spectrum framework that is essential to understanding such dynamic processes [15].

$$\Phi_n(\vec{k}) \simeq 0.033 C_N^2 K^{-\frac{11}{3}} \quad (1)$$

Where:

$\Phi_n(\vec{k})$ represents the Kolmogorov power spectrum.

C_N^2 represents the measure of strength regarding refractive index fluctuations.

K denotes spatial frequency.

The parameter C_N^2 reveals significant variability, spanning from approximately $10^{-17} m^{2/3}$ or lower in milder atmospheric situations to roughly $10^{-13} m^{2/3}$ or higher in stronger conditions. These fluctuations often result in peak values during midday, relatively stable readings throughout the night, and troughs around sunrise and sunset. This recurring daily

pattern, marked by the lowest values at these times, is frequently referred to as the diurnal cycle.

1-The fidelity criteria

There is an explanation and equation for Root Mean Squared Error (RMSE), Variance, Strehl Ratio, and Correction Rate:

1.1 Root Mean Squared Error (RMSE):

The average magnitude of errors between the actual and predicted values is measured by RMSE [16].

$$RMSE = \sqrt{\frac{1}{N}\sum_{i=1}^{N}(x_i - y_i)^2} \quad (2)$$

Where x_i is the observed value and y_i is the predicted value.

1.2 Variance:

Variance measures the spread or dispersion of a set of data points [17].

$$Variance = \frac{1}{N}\sum_{i=1}^{N}(x_i - \mu)^2 \quad (3)$$

Here, μ is the mean of the data set.

1.3.Strehl Ratio:

An optical system's or wavefront's quality is indicated by the Strehl ratio. It can be specified as the ratio between the ideal, diffraction-limited wavefront's peak intensity as well as the aberrated wavefront's peak intensity. The Strehl ratio equation is [18]:

$$Strehl\ Ratio = \frac{I_{aberrated}}{I_{diffraction-limited}} \quad (4)$$

Where:

- $I_{aberrated}$ is the peak intensity of an aberrated wavefront.
- $I_{diffraction\text{-}limited}$ is the peak intensity of the ideal, diffraction-limited wavefront.

1.3Correction Rate:

The Structural Similarity Index (SSI) is an evaluation metric designed to gauge the similarity between two images. It provides a thorough evaluation by taking into account both luminance and structural properties, which enables it to identify perceived changes in images that go beyond minor variations in pixel values. SSI provides a sophisticated evaluation of similarities by taking into account the overall image structure, luminance, and contrast through the analysis of local patterns of pixel intensities. The SSI formula is commonly expressed as follows [19, 20, 21]:

$$SSI(x,y) = \frac{2\mu_x\mu_y + c_1}{\mu_x^2 + \mu_y^2 + c_1}\frac{2\sigma_{xy} + c_2}{\sigma_x^2 + \sigma_y^2 + c_2} \quad (5)$$

Where:

- x and y represent the compared images.
- μ_x and μ_y represent the means of x and y.
- σ_x^2 and σ_y^2 represent the variances of x and y.
- σ_{xy} represents the covariance of x and y.
- c_1 and c_2 represent the constants added to avoid instability when the means and variances approach zero. To get an overall similarity value, SSI is often computed over a number of local patches in the images and, after that, averaged.

2.Results and Discussion

The first step of the simulation models the dynamic behavior of solar granulation using cellular automata techniques. By simulating the formation and progression of granules

alongside the intergranular lanes, this approach delves into the intricate processes unfolding on the solar surface.

A numerical computer simulation was conducted to investigate the effectiveness of Zonal AO systems for correcting wavefronts. Additionally, a phase screen was created to replicate the statistical characteristics of phase fluctuations caused by turbulent atmospheric conditions, utilizing a Kolmogorov model. The numerical simulation results for the profiled wavefront beam propagation across the turbulent medium (atmosphere) are shown in this section.

1. Initialization and Parameter Setup

- Define simulation parameters, number of grid points per each side, total size of the grid (m), grid spacing (m), atmospheric turbulence strength, number of actuators in the deformable, maximum stroke of the deformable mirror, number of time steps, Deformable Mirror (DM), and Point Spread Function (PSF) Generation:

1- Generate an amplitude pattern (circular deformable mirror (DM) aperture) for the wavefront, as in Figure 1.

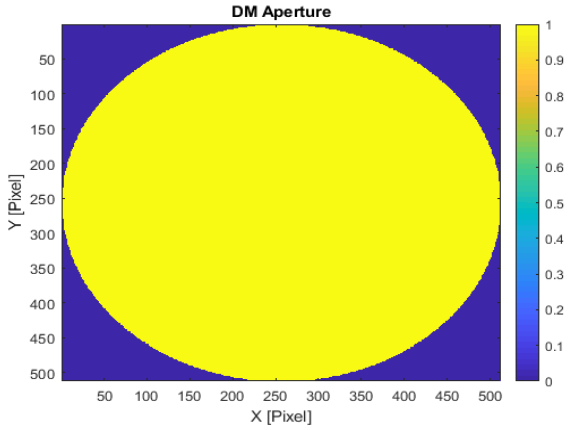

Figure 1: DM Aperture.

2.Simulation of Solar Granules' Steps

1. Grid Representation: The simulation uses a grid where each cell represents a portion of the sun's surface. The state of each cell is either 'granule' (1) or 'non-granule' (0).

2. Initialization: The initial state of the grid is set randomly, where cells are designated as granules or non-granules based on a random probability threshold.

3.Simulation Rules:

a. **Neighborhood Influence:** Granules evolve based on their local environment, which is determined by their neighboring cells.

b. **Granule Growth or Disappearance:** Depending on the states of its neighboring cells, rules are used to determine if a granule should remain the same, expand, or disappear during each iteration.

4.Iteration:

a. The simulation progresses through multiple iterations (time steps), where the state of each cell is updated based on the defined rules.

b. For each iteration, a new grid (next Granules) is generated to represent the updated state of granules according to the rules.

c. After each iteration, the current state of the grid is visualized to show the evolving granulation pattern.

5.Visualization:

The simulation of solar granules utilizes a cellular automaton-based approach to model the dynamic behavior of granules (Figure 2). The dynamics revealed patterns of growth and movement, influenced by local neighbor interactions and specific rules, leading to an evolving granular structure.

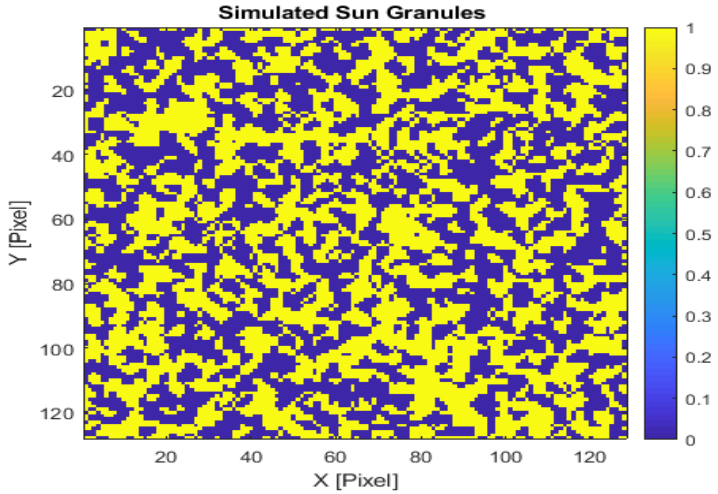

Figure 2: Solar Granulation Simulation

.

d.Wavefront Distortion

The initial distorted wavefront, induced by atmospheric turbulence, demonstrates the presence of aberrations and phase distortions. The effect of a distorted wavefront on the original image (solar granulation) can be shown in Figure 3.

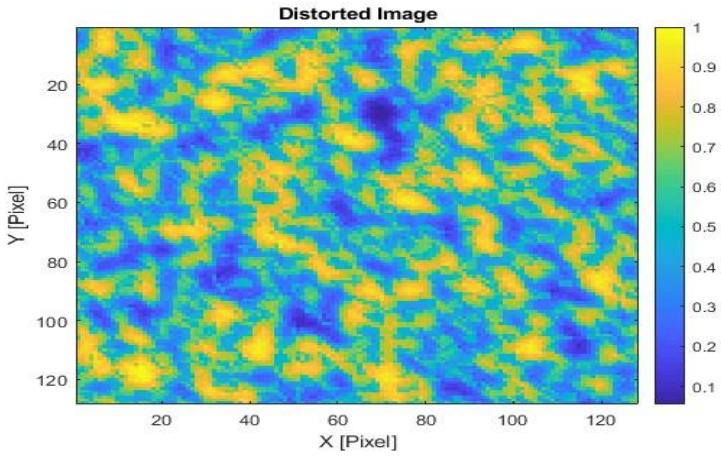

Figure 3: Distorted Image

c. Wavefront Reconstruction and the Influence Matrix

The influence matrix represents the interaction of deformable mirror actuators with the wavefront. The influence matrix function is used to generate an influence matrix for Zonal AO, as in Figure 4. In zonal AO, a deformable mirror is divided into multiple small segments, or actuators, and each actuator can be controlled independently to correct the wavefront distortions introduced by atmospheric turbulence. The influence variable is calculated by applying a Gaussian-like influence profile centered at the actuator's position on the wavefront grid. This

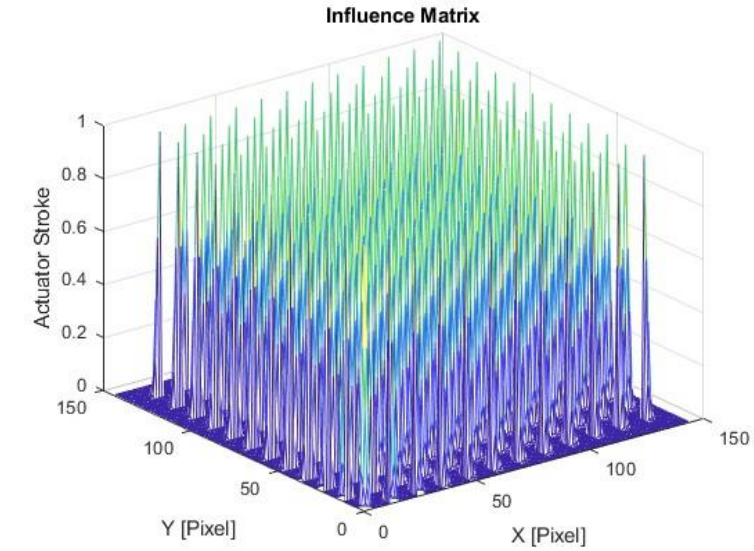

Figure 4: Influence Matrix

profile describes how an actuator affects nearby pixels.

The result of Zonal AO compensation can be shown in Figures 5-6, by reconstructing the distorted wavefront as a corrected wavefront.

d.Point Spread Function (PSF) Analysis

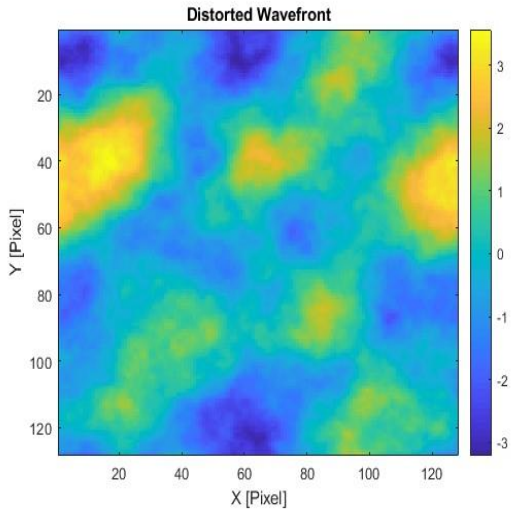

Figure 5: Distorted

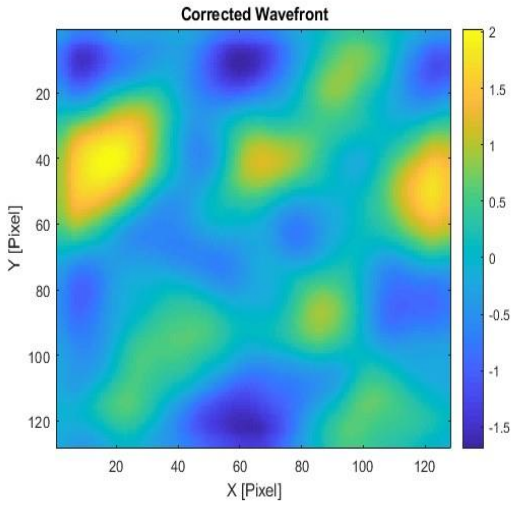

Figure 6: Corrected

The Point Spread Function without atmospheric turbulence (Figure 7) showcases the ideal PSF, whereas the PSF with turbulence (Figure 8) exhibits distortions due to the turbulent

atmosphere. The reconstructed PSF after applying Zonal AO correction (Figure 9) displays notable improvements, approaching the ideal PSF.

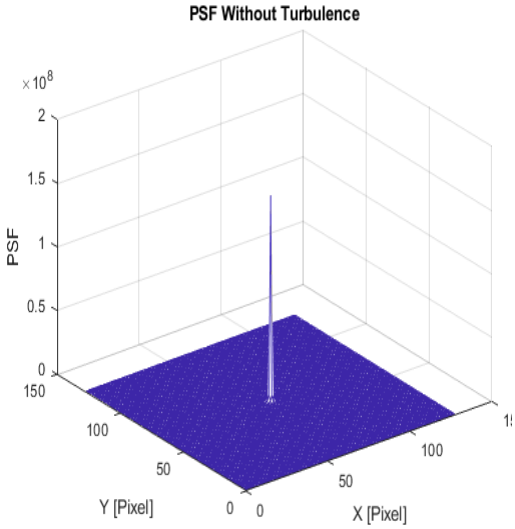

Figure 7: PSF without

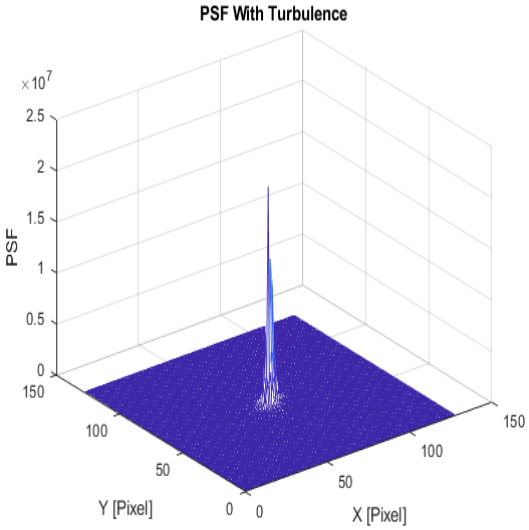

Figure 8: PSF with

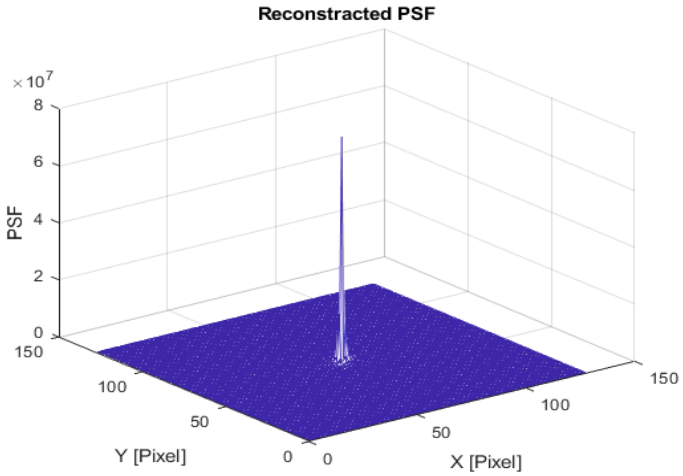

Figure 9: Reconstructed PSF after Zonal AO

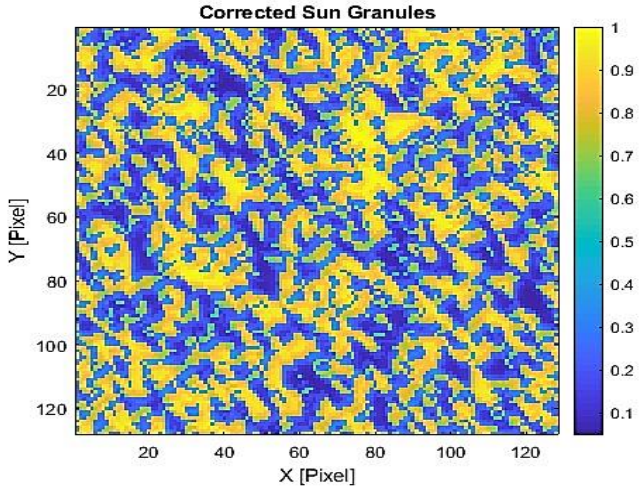

Figure 10: The corrected sun's

Utilizing the corrected PSF, image reconstruction was conducted on the original sun's granules (Figure 2). The corrected image (Figure 10), compared to the distorted image (Figure 3), demonstrates a significant enhancement in visualized image quality, particularly in restoring

finer details and reducing distortions caused by atmospheric turbulence.

d. Additional Visualization and Analysis

Figure 11 illustrates the Strehl Ratio concerning different atmospheric turbulence strengths. As expected, the Strehl Ratio decreases as the atmospheric turbulence strength increases. This reduction is due to increased aberrations and distortion caused by stronger atmospheric turbulence, impacting the system's ability to correct for these distortions effectively. The observable decline in the Strehl Ratio indicates the system's decreased efficiency incorrecting optical aberrations

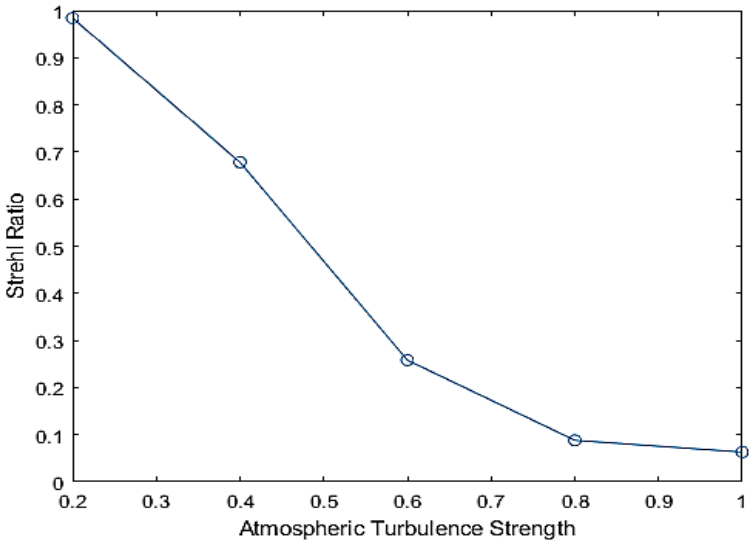

Figure 11: The Strehl Ratio as a Function of Atmospheric Turbulence Strength

The plotted Figures (12-14) show various performance metrics concerning an AO system at different atmospheric turbulence strengths.

The RMSE, normalized for comparison, indicates the precision of the adaptive optics system in correcting aberrations. A higher RMSE suggests increased residual errors after correction. As the atmospheric turbulence strength increases, the RMSE rises, demonstrating that higher turbulence levels challenge the system's ability to minimize errors and improve image quality (Figure 12).

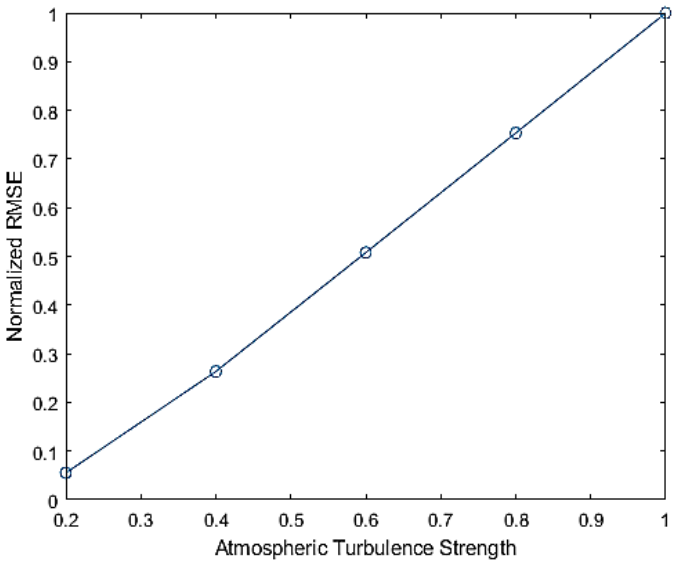

Figure 12: RMSE vs. Atmospheric Turbulence Strength

The correction rate (SSI) plot displays the system's speed in correcting distortions induced by atmospheric turbulence (as in Figure 13). The decline in correction rate with higher turbulence strength indicates that the system takes more time to correct distortions as turbulence increases. This could be due to an increased complexity in the correction process under stronger atmospheric disturbances.

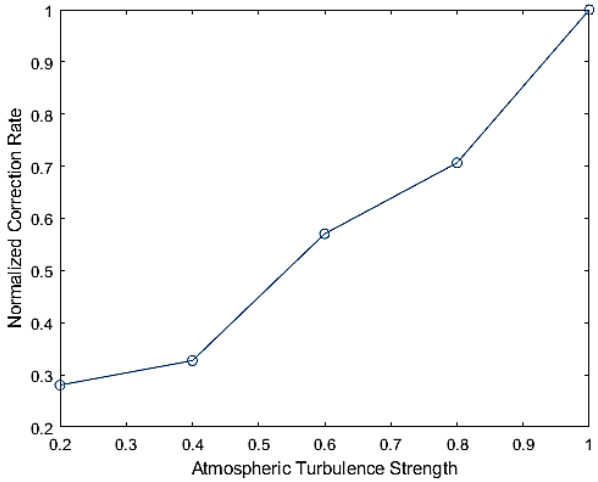

Figure 13: Correction rate vs. atmospheric turbulence strength

Figure 14 exhibits the normalized variance, portraying the stability of the correction across different pixel positions. The legend differentiates the stability concerning varied atmospheric turbulence strengths. A less fluctuation curve signifies more uniform correction stability across pixels. The Figure suggests that as the atmospheric turbulence strength increases, the uniformity of correction stability tends to decrease, indicating challenges in maintaining stability in correcting aberrations uniformly across the image.

Overall, these figures collectively indicate the adaptive optics system's performance under varying atmospheric turbulence strengths, showcasing its ability to correct distortions, the precision achieved, the speed of correction, and the uniformity of correction stability across

different conditions.

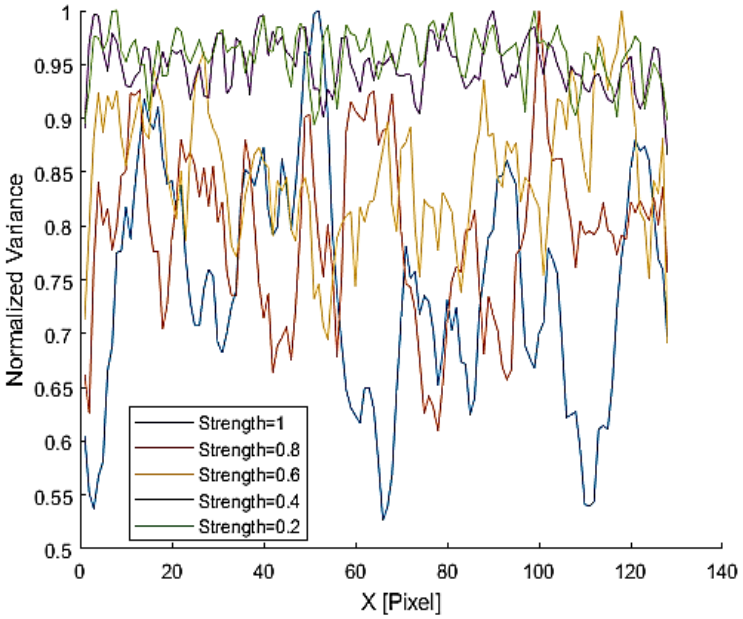

Figure 14: Normalized Variance (Correction Stability) vs. Pixel Position

3.Conclusion

Comprehensive simulation results demonstrate the effectiveness of the Zonal AO system in reducing atmospheric turbulence-induced wavefront distortions. The simulation of solar granulation using cellular automata clarifies dynamic granular patterns. The corrected PSF and improved image reconstruction highlight the significant improvement in the wavefront achieved by the Zonal AO correction approach under weak turbulence conditions. However, a decrease in the Strehl ratio and an increase in RMSE indicate the challenge of maintaining high precision in the presence of greater atmospheric turbulence.

Furthermore, the results reveal a weakness in the Zonal AO system's ability to treat high distortions in the wavefront, as evidenced by the decrease in Strehl ratio values from 0.98 to 0.085 for disturbance strength values from 0.2 to 1, respectively. Additionally, as turbulence strength increases, the uniformity of correction stability across pixels decreases, and the correction rate falls, possibly due to increased complexity in the distortion correction process.

In summary, these findings underscore the system's robustness while confirming the challenges posed by intense atmospheric disturbances. This information is crucial for the improvement of Zonal AO systems in solar imaging applications.

References

[1] R. N. Hassan, H. S. Ali, and W.H. Wadee, "Computer Simulation for the Effects of Optical Aberrations on Solar Images Using Karhunen-Loeve Polynomials", *Iraqi Journal of Science*, Vol. 62, No. 7, PP. 2463-2473, 2021. DOI: https://doi.org/10.24996/ijs.2021.62.7.35.

[2] T. Roudier, M. T. Eibe, J. M. Malherbe, M. Rieutord, P. Mein, N. Mein and M. Faurobert, "Temporal height properties of the exploding granules", *Astronomy & Astrophysics*, Vol.368, No. 2, PP. 652-661, 2000. https://doi.org/10.1051/0004-6361:20000511.

[3] M.M. Zamal , M.N.Al Najm, " Computation of the Relationships of X-ray to Radio Luminosities of a Sample of Starburst Galaxies", *Iraqi Journal of Science* , Vol. 64, No. 6, PP. 4076–4093, 2023. https://doi.org/10.24996/ijs.2023.64.6.44

[4] H. S. Ali, "Performance Estimation of Solar Imagery Using Different Types of Atmospheric Turbulence Models", *Iraqi Journal of Science*, Vol.64, No. 7, PP: 4579-4590, 2023. https://doi.org/10.24996/ijs.2023.64.7.43

[5] A. H. Al-Hamadani, F. S. Zainulabdeen, G. S. Karam, E. Y. Nasir, and A. Al-Saedi, "Effects of Atmospheric Turbulence on the Imaging Performance of Optical System", *AIP Conf. Proc.*, Vol. 1968, A030071, 2018. https://doi.org/10.1063/1.5039258

[6] R.F.H. Foadi, and A.K. Ahmed, "Designing Cassegrain Telescope System with Best Obscuration Ratio of Secondary Mirror". *Iraqi Journal of Science*, Vol. 64, No. 12, PP. 6638–6647, 2023. DOI:10.24996/ijs.2023.64.12.42

[7] R. N. Hassan, and H.S. Ali, "performance estimation and system modeling for refractive index structure constant Cn2". *Karbala International Journal of Modern Science*, Vol. 9, No. 2, PP. 178-186, 2023. https://doi.org/10.33640/2405-609X.3291.

[8] S. U. Jasim , and R. N. Hassan ,"Investigation of Numerical Simulation for Adaptive Optics System". *Iraqi Journal of Physics*,Vol. 21 No. 3, PP. 9-23, 2023. https://doi.org/10.30723/ijp.v21i3.1122

[9] M. Mirdan, R. N. Hassan, and B. Al-Abudi, "Performance Simulation for Adaptive Optics Technique Using OOMAO Toolbox", *Karbala International Journal of Modern Science*, Vol.8, Issue.3, PP. 306-312, 2022.DOI.org/10.33640/2405-609X.3233

[10] R. Kamlah, M. Verma, C. Denker and H. Wang, "High-Resolution Imaging of Solar Pores", Astronomy & Astrophysics, Vol. 675, A182, PP. 1-16, 2023. https://doi.org/10.1051/0004-6361/202245410

[11] Y. X. Liu, C.W. Jiang, D. Yuan, P. B. Zuo and W.D. Cao, "Length Scale of Photospheric Granules in Solar Active Regions", *Research in Astronomy and Astrophysics*, Vol. 22, No. 8, PP. 1-8, 2022.**DOI** 10.1088/1674-4527/ac7518.

[12] A.G. Hoekstra, J. Kroc, and P.M.A. Sloot, "Simulating Complex Systems By Cellular Automata", 2nd ed., SpringerLink: Berlin, Germany, 2018, 657–689, ISBN 3642122035. [**Google Scholar**].

[13] M. Czarnecki, M. Sitko, and Ł. Madej, "The Role of Neighborhood Density in the Random Cellular Automata Model of Grain Growth", *Computer Methods in Materials Science*, Vol. 21, PP. 129–137, 2021. https://doi.org/10.7494/cmms.2021.3.0760

[14] M. Lamb, C. Correia, S. Sivanandam, R. Swanson, and P. Zavyalova, "Simultaneous Estimation Of Segmented Telescope Phasing Errors and Non-Common Path Aberrations From Adaptive Optics Corrected Images", *Monthly Notices of the Royal Astronomical Society*, Vol. 505, Issue 3, Pages 3347–3360, 2021.https://doi.org/10.1093/mnras/stab1247

[15] W. Zou, "Optimization of Zonal Wavefront Estimation and Curvature Measurements", Electronic Theses and Dissertations, University of Central Florida, Orlando, United States, 2007.

[16] H. Wang, Z. Yang, L. Liu, Y. Chen, F. Wang, and Ya. Cai, "Orbital Angular Momentum Spectra of Twisted Laguerre-Gaussian Schell-Model Beams Propagating in Weak-To-Strong Kolmogorov Atmospheric Turbulence", *Optics Express*, Vol. 31, Issue 2, PP. 916-928,2023. https://doi.org/10.1364/OE.477029,

[17] T. Chai and R. R. Draxler, "Root mean square error (RMSE) or mean absolute error (MAE)? Arguments against avoiding RMSE in the literature", *Geoscientific Model Development* Vol.7, No. 3, PP.1247-1250, 2014. https://doi.org/10.5194/gmd-7-1247-2014

[18] J. I. Watling, L. A. Brandt, D. N Bucklin, I. Fujisaki , F.J. Mazzotti, S. S. Romañach, and C. Speroterra, "Performance metrics and variance partitioning reveal sources of uncertainty in species distribution models", *Ecological Modelling*, Vol. 309, PP. 48-59, 2015. https://doi.org/10.1016/j.ecolmodel.2015.03.017

[19] L. Labate, P. Ferrara, L. Fulgentini, and L. A. Gizzi, "Effects of small misalignments on the intensity and Strehl ratio for a laser beam focused by an off-axis parabola", Applied Optics, Vol. 55, Issue 23, PP. 6506-6515, 2016. https://doi.org/10.1364/AO.55.006506

[20] J. Yao , J. Shen , and C. Yao, "Image Quality Assessment Based On The Perceived Structural Similarity Index Of An Image", *Mathematical Biosciences and Engineering*, Vol. 20, No. 5, PP. 9385-9409. 2023. Doi: 10.3934/mbe.2023412.

[21] A. H. Baker, A. Pinard, and D. M. Hammerling, "On a Structural Similarity Index Approach for Floating-Point Data", *IEEE Transactions on Visualization and Computer Graphics*,Vol. 2, PP. 1-12, 2023. DOI: 10.1109/TVCG.2023.3332843.